ELSEVIER

Materials Science and Engineering B 149 (2008) 259–265

MATERIALS SCIENCE & ENGINEERING B

www.elsevier.com/locate/mseb

Photonic band gap materials in butterfly scales: A possible source of "blueprints"

K. Kertész [a], G. Molnár [a], Z. Vértesy [a], A.A. Koós [a], Z.E. Horváth [a], G.I. Márk [a], L. Tapasztó [a], Zs. Bálint [b], I. Tamáska [a], O. Deparis [c], J.P. Vigneron [c], L.P. Biró [a,*]

[a] *Research Institute for Technical Physics and Materials Science, POB 49, H-1525 Budapest, Hungary*
[b] *Hungarian Natural History Museum, Baross utca 13, H-1088 Budapest, Hungary*
[c] *Facultes Universitaires Notre Dame de la Paix, Rue de Bruxelles 61, B-5000 Namur, Belgium*

Received 25 June 2007; received in revised form 5 October 2007; accepted 9 October 2007

Abstract

The color generating nanoarchitectures in the cover scales of the blue (dorsal)–green (ventral) wing surfaces of the butterfly *Albulina metallica* were investigated by scanning electron microscopy and cross-sectional transmission electron microscopy. A layered, quasiordered structure was revealed in both the dorsal and ventral scales, with different order parameters, associated with their different colors. A successful attempt was made to reproduce the biological structure in the form of a quasiordered composite (SiO/(In & SiO)) multilayer structure using standard thin film deposition techniques. The position of the reflectance maxima of this artificial structure could be tailored by controlling the size of the In inclusions through oxidation. Our results show that photonic band gap materials of biologic origin may constitute valuable blueprints for artificial structures.

Keywords: Photonic crystals; Butterfly scales; Bioinspired nanoarchitectures; Quasiordered multilayers; Reflectance; Tuning by oxidation

1. Introduction

Electron waves in the periodic potential of a crystal are arranged into energy bands separated by gaps where propagating states are prohibited. A semiconductor has a complete band gap between the valence and the conduction energy bands. It is now known that analogous band gaps can exist when electromagnetic (EM) waves propagate in periodic dielectric structure, i.e., in a composite with regular, one- (1D), two- (2D), or three-dimensional (3D) structure, made of two materials with different refractive indexes, $n_1 \neq n_2$ [1–3]. The difference $(n_1 - n_2)$ is called the refractive index contrast of the photonic crystal (PhC), named so on the basis of analogy with the atomic crystalline structure of solids exhibiting band gaps for electrons.

A PhC will have wavelength ranges in which the EM radiation cannot propagate through the structure [3]. These wavelength ranges are called stopbands and the materials having stopbands are also referred to as photonic band gap (PBG) materials. Such materials were introduced into the focus of the scientific community following the work of Yablonovitch [1] and of John [2]. In the past 20 years continuously growing efforts were focused on the practical realization and theoretical understanding of PBG materials due to their many potential applications ranging from photonic computing [3,4] to new, environmentally friendly colorants [5].

For a PhC with PBG in the wavelength range of the visible light, the typical periodicity of the composite has to be in the range of 100 nm. Therefore, these structures are nanoarchitectures, most frequently 3D nanoarchitectures with complex structure, constituting a technological challenge even nowadays [6]. Frequently, the nanoarchitectures realized first by e-beam lithography or by colloidal assembly are transformed often by several tedious and costly steps of infiltration, atomic layer deposition, oxidation, etc., to achieve the increase of the refractive index contrast of the composite to values in the range of 2–3, or to transform a direct opal into an inverse one [4,7].

The physics and materials science community became only recently aware that similar PBG structures were developed by several species of butterflies in order to produce color for sexual communication [8–10], cryptic behavior [10], or the PBG materials may have role in thermal management, too [11]. It is

* Corresponding author. Tel.: +36 1 3922681; fax: +36 1 3922226.
E-mail address: biro@mfa.kfki.hu (L.P. Biró).
URL: http://www.nanotechnology.hu/ (L.P. Biró).

0921-5107/$ – see front matter © 2007 Elsevier B.V. All rights reserved.
doi:10.1016/j.mseb.2007.10.013

quite remarkable that these nanoarchitectures are built of chitin ($n = 1.58$) and air, i.e., at a rather moderate refractive index contrast. The butterfly wing scales in which the color producing nanoarchitectures are located have typical thicknesses in the micron range, still some butterflies, like the blue nymphalid *Morpho rhetenor* and its congeners are so conspicuous, that their blue flashing can be noticed by the naked eye from several hundreds of meters away [8]. Apparently, natural evolution found clever ways to produce very efficient PBG materials at a moderate refractive index contrast, close to that which could be achieved between air and the widely used photoresists. The introduction of the natural "blueprints" may reveal new paths for the development of the artificial PhCs.

Another interesting direction in which bioinspiration may open up new pathways in PBG material research concerns the quasiordered structures. Often, the biologic PBG materials lack that very rigorous order which is demanded in artificial structures [6], still they can generate conspicuous colors, sometimes even with metallic glance. Although these quasiordered systems are unlikely to find application in photonic computing, they may reveal useful ideas for colorants, coatings and perhaps for textile and paper industry, too. The more so, that the practical realization of such structures, may be a lot less demanding than that of structurally perfect PhCs with band gap in the visible range.

In the present paper we investigate the nanoarchitectures producing the colors of the blue (dorsal)–green (ventral) wings of the butterfly *Albulina metallica* (Felder and Felder, 1865) (Lepidoptera: Lycaenidae) (Fig. 1) living in high altitude open habitats in the Himalaya mountains and we make an attempt to reproduce the observed quasiordered structures by thin film deposition.

The butterfly wings are covered by scales built of chitin, the scales may have a rather intricate nanoarchitecture [12]. Their typical dimensions are in the range of 50 μm × 150 μm with thickness in the micron range. Scales are the cuticular product of one single cell. Usually each side of the wings of butterflies is covered by two distinct layers of scales: one closer to the wing membrane (ground scales) and one closer to the wing surface (cover scales) [13]. Most frequently the source of color lies in the cover scales, for *A. metallica* we tested that the cover scales are the ones responsible for coloration [14].

Fig. 1. Photographs of the butterfly *Albulina metallica* (left: dorsal view, right: ventral view). On the ventral surface only the hindwing exhibits shiny, silver–green structural color, the light brown of the forewing has pigmental origin. (For interpretation of the references to color in this figure legend, the reader is referred to the web version of the article.)

2. Experimental results and discussion

The micro- and nanoarchitecture of the color producing scales of the *A. metallica* were investigated by various microscopic methods: optical microscopy, scanning electron microscopy (SEM) and transmission electron microscopy (TEM). For SEM samples wing pieces were cut and coated with 20 nm Au prior to examination, in order to avoid charge buildup. TEM samples were prepared by incorporating wing pieces in EMbed 812 resin and cut using ultramicrotome. The optical properties were revealed by reflectance measurements of complete wings [15] and reflectance and transmission measurements performed on single scales [16]. The optical measurements on butterfly wings and scales were carried out using an Avaspec 2048/2 fiber-optic spectrometer, both in specular arrangement under normal incidence and using a 3-cm integrating sphere in order to collect all the light reflected under any angle of emergence. All optical measurements were carried out with non-polarized light. For the butterfly wings and scales an Avaspec diffuse, white standard was used as comparison sample for reflection measurements, while for the artificial multilayers an Ocean Optics high-reflectivity specular reflectance standard was used. The single scale measurements were carried out by combining the fiber optic spectrometer with an optical microscope.

The reflectance measurements on wing pieces showed that the dorsal wing surface gives two normal incidence reflectance maxima, close to each other, at 415 and 450 nm, respectively, while the measurement with the integration sphere yielded one single, broad maximum at 416 nm. On the ventral side the normal incidence reflectance maximum was found at 560 nm and in the measurement with the integration sphere at 545 nm [15]. Stripping layer by layer the scales from butterfly wings and single scale measurement clearly showed: the cover scales are indeed the ones, which are responsible for the coloration of both wing surfaces [14,16].

The nanoarchitecture of the cover scales as revealed by SEM (in the plane of the scale) and by TEM (in plane transversal to the plane of the scale) is shown in Figs. 2 and 3, respectively. One may observe in Fig. 2 that the nanoarchitectures do not show a regular structure with long range order. However, the distance of the first neighbors of the holes seen in the plane of the scale – the so called "pepper-pot structure" [10] – is constant. In order to study local order in the SEM images of quasiordered butterfly scales, we have developed a nonlinear direct space algorithm, based on averaging the local environment of the holes. The method provides the statistical distribution of the local environments, including the histogram of the nearest neighbor distance and the number of nearest neighbors. This algorithm was integrated in the BioPhot Analyzer

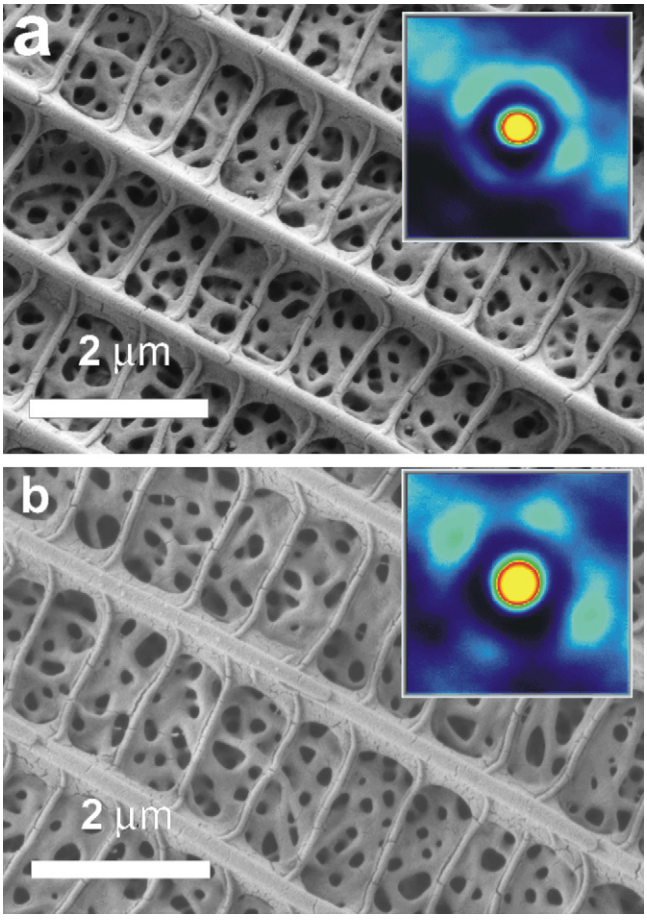

Fig. 2. SEM images of the cover scales on the dorsal (a) and ventral (b) surfaces of the wings of *A. metallica*. The insets in the upper, right corner show the averaged vicinity of holes (>2000 holes averaged) [17], both insets have an area of 800 nm × 800 nm. It can be clearly seen that the hole size and the distribution of the first neighbor holes is different for the dorsal and the ventral scales. (For interpretation of the references to color in this figure legend, the reader is referred to the web version of the article.)

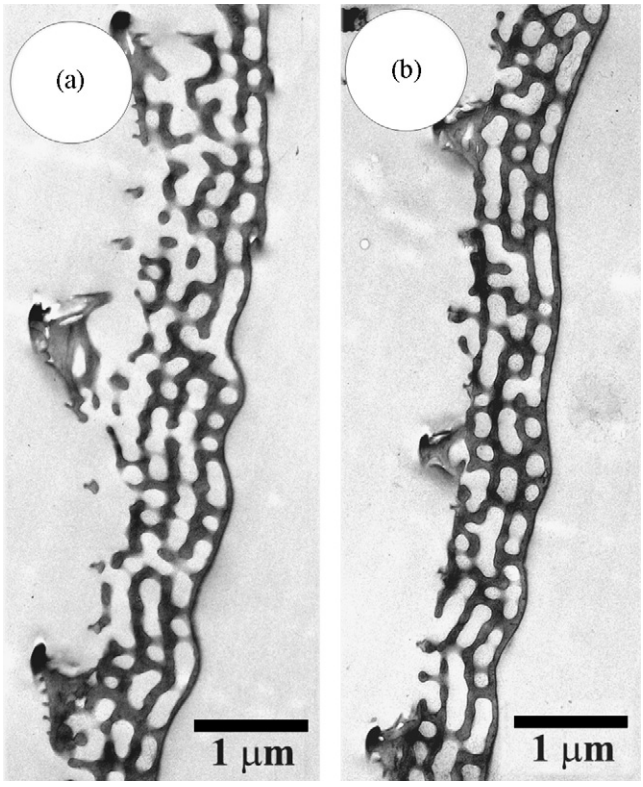

Fig. 3. Cross-sectional TEM images of the dorsal (a) and ventral (b) cover scales of *A. metallica*, section thickness 70 nm. *Note*: The presence of filled layers separated by compositee layers (chitin and air).

software, as part of its unique toolbox optimized for quantitative investigation of SEM and TEM images of butterfly scales. [14,17]. The averaged hole diameters, the distribution of the holes in the first neighborhood and the characteristic distance between the first neighbors are shown in the insets in the upper right hand corner of the SEM images. These clearly show that the hole size and the distances between holes differ in the two types of scales, which must be the reason of difference in their coloration.

The quasiordered character of the scales of *A. metallica* is in contrast with what was found in the case of *Cyanophrys remus* (Hewitson, 1868) (Lepidoptera: Lycaenidae), where the hole pattern exhibited long range ordering, in other words, it was a single crystal in the full sense of the word, as demonstrated by Fourier analysis, too [10]. At a first glance, it is surprising that such a disordered structure as found in the scales of *A. metallica*, can generate color like a highly ordered one [10,15]. On the other hand in an earlier work, we already showed that not fully ordered structures are responsible for the coloration of many lycaenid butterfly species with blue wing surfaces [11].

TEM images in Fig. 3, show that in a plane normal to the plane of the scale the typical structure is constituted from mostly continuous, filled layers, separated by layers where filled and empty regions (matrix and filler) alternate in an apparently random way. In the interpretation of the TEM images of such a thin slice of a complex nanoarchitecture several aspects have to be taken into account [10]. In the case of *A. metallica*, one has to be aware that due to the finite thickness of the cross-section (70 nm) the tiny pillars joining two consecutive continuous layers may appear missing. This finding is supported by the examination of many independent sections and in each section of many scales that were sectioned. So, the somewhat simplified structural model resulted from combining SEM and TEM data for the cross-section of such a scale will be like the one shown in Fig. 4a. In Fig. 4b a more disordered structure is presented in which even the thickness of the layers separating the composite layers was made random. This second structure is very clearly different from what one would call a 1D photonic crystal, or a Bragg reflector, on the other hand it can be quite conveniently achieved practically.

In order to try to "mimic", (without reproducing it exactly) in an artificial structure the quasiordered PBG type material found in the scales of *A. metallica* we took a simple approach as detailed below.

The system SiO/(In & SiO) was chosen to investigate the optical behavior of disordered composite multilayer structures similar to that shown in Fig. 4b. This choice was motivated by the possibility to oxidize In under relatively mild conditions

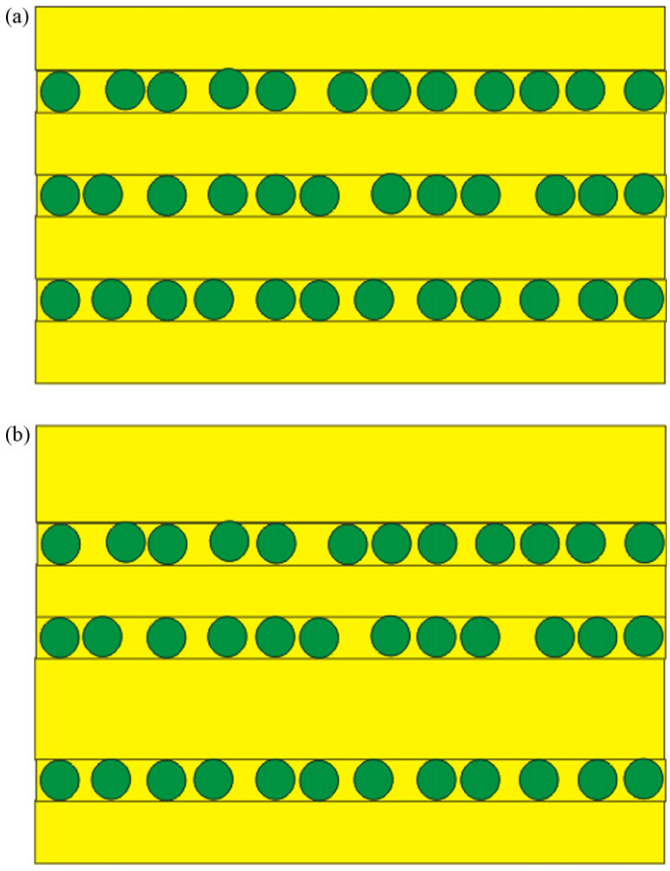

Fig. 4. Model of the layered, quasiordered structure found in the scales of *A. metallica* (a). Model of an artificial structure with added disorder in layer thickness (b). Different colors (shades of grey) correspond to different refractive indexes. Drawings not to scale. (For interpretation of the references to color in this figure legend, the reader is referred to the web version of the article.)

which do not modify the SiO layer (in air at 300 °C). The oxide (In_2O_3) has an index of refraction of $n = 1.9$, close to that of SiO, so that the oxidation can be regarded as a procedure to tailor the size of In particles without inducing major modifications in other components of the system. To introduce a further factor of disorder, additional to the random arrangement of In particles in the SiO matrix, the distance between the composite layers (In & SiO filling) was chosen to vary randomly as seen in Fig. 4b and the cross-sectional SEM image in Fig. 5a. Both SiO and In were deposited successively by standard thin film techniques in the same evaporation installation. The In particles had typical diameters in the range of 50 nm and had spherical shape as shown in Fig. 5b. The complete multilayer has the structure detailed in Table 1. The presence of In particles in each composite layer is clearly revealed by the top view SEM image of a cleaved sample, Fig. 5c.

Taking the average particle diameter to be 50 nm and an average spacing between particles of 20 nm (Fig. 5 and top view SEM images of single layers not shown in the paper) the volume filling fraction in the composite layers (In volume/total volume) can be calculated to be 0.19.

The oxidation process was monitored by X-ray diffraction (XRD). The measurements showed that in the as-grown sam-

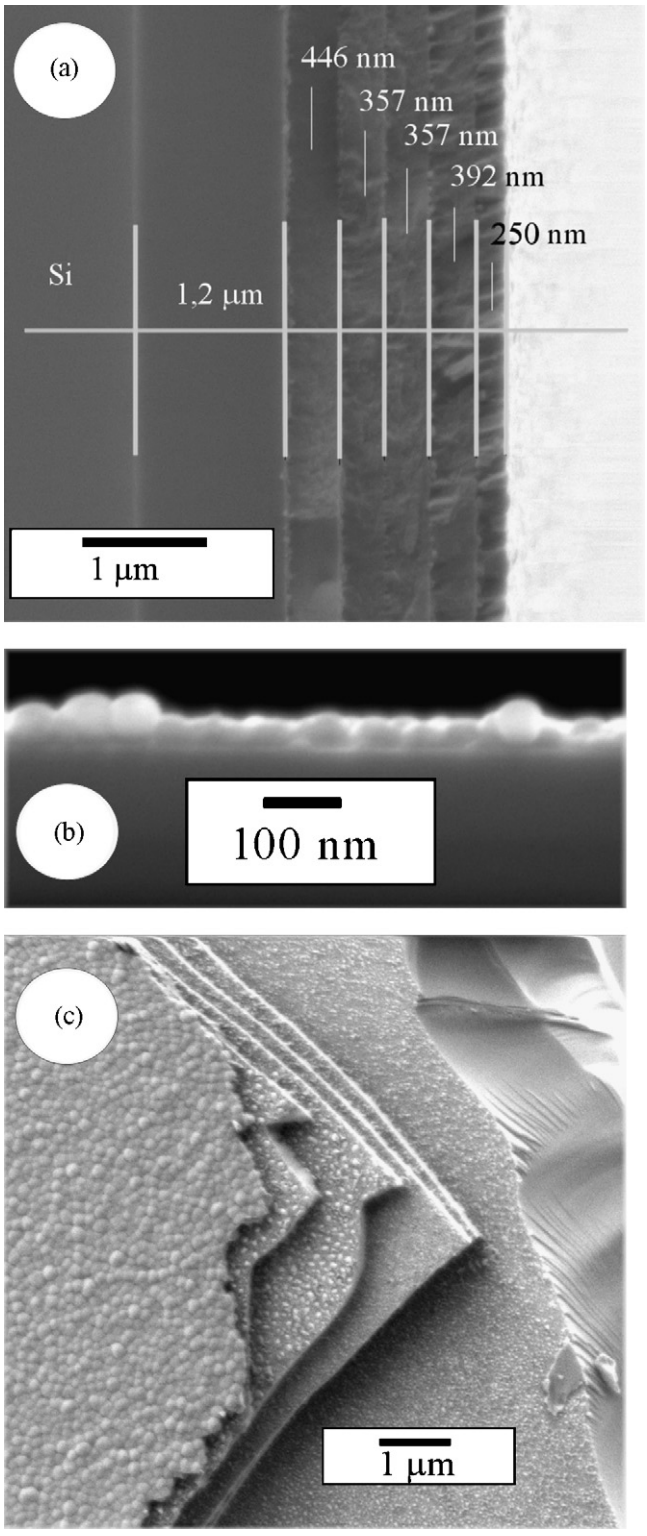

Fig. 5. Artificial layered structure of SiO/(In & SiO). (a) Cross-sectional SEM image showing the arrangement and thicknesses of the layers. (b) Cross-sectional SEM image of one single In layer on SiO. One may note the spherical particle shape and diameters in the range of 50 nm. (c) Top view SEM image of the broken multilayer structure, clearly showing steps at each individual (In & SiO) layer.

Table 1
Structure of the quasiordered multilayer system produced to mimic the structures revealed by electron microscopy in the scales of *Albulina metallica*

Layer	Thickness (nm)	Observations
Si	–	Substrate
SiO_2	1200	Standard, semiconductor quality, thermal oxide
In and SiO	50	
SiO	446	
In and SiO	50	
SiO	357	
In and SiO	50	
SiO	357	
In and SiO	50	
SiO	392	
In and SiO	50	
SiO	250	Cover layer

ple only very weak indium oxide traces were present. After the 30 min of annealing at 318 °C in air, the height of the In peak was reduced to half of its initial value and a strong In_2O_3 peak appeared, Fig. 6. Taking into account that the area under the XRD peak can be regarded as proportional to the volume of the material present, it can be estimated from the XRD data that roughly half of the In volume in the as-grown multilayer was converted to crystalline indium oxide. In other words the volume filling fraction of In in the composite layers (In, SiO, In_2O_3) was reduced to 0.09. Although chemically different, the In_2O_3 has a similar refractive index like SiO, so that in the first approximation the optical behavior of the composite layer after oxidation is mainly determined by the reduction of the size of In particles.

The optical behavior of the samples was characterized by normal incidence reflectance measurements, shown in Fig. 7, both in as-grown and oxidized state. The major peak of the as-grown structure can be regarded as being positioned at 754 nm. Two smaller peaks appear at 410 and 570 nm. After the oxidation step the main peak was shifted to 700 nm the secondary peak in the range of 500 nm has vanished, the third peak was shifted to 380 nm and strongly reduced in amplitude. All of these changes may be associated with the reduction of the size of randomly arranged grains due to oxidation, as it will be made clear from simulations results discussed later. These finding shows that indeed, such structures with a fairly high degree of disorder, both in layer thickness and the indium particle distribution in the composite layers, can produce reflectance maxima, i.e., color. The position and intensity of these maxima can be tailored by controlling only the particle size without significantly altering other geometric parameters of the multilayer structure. This confirms the observation from the SEM images in Fig. 2, where the insets showing the averaged hole diameters and the averaged distance to the first neighbors suggested that the observed difference in the coloration of the two kinds of scales arises from the differences in the hole diameter and the distance to the first neighbors. The oxidation treatment did not modify the distance at which the optically different inclusion are placed—as the centers of the particles did not change position, but modified their size, like shown in the model in Fig. 8. The two darker bands above and below each composite layer (In & SiO) correspond to the thickness with which the widths of the oxide-only layers were modified by the oxidation. As this modification can be estimated to be of the order of 10–25 nm, it corresponds to less than 10% alteration of the oxide (SiO plus In_2O_3) layer thickness, which is not expected to give very significant differences taken into account that the as-grown individual layer thicknesses differ by as much as 28%. So, the modification of the reflectance spectra is attributed to the reduction of the size of the optically different inclusion.

To get more insight in the modification of the optical properties of the bioinspired quasiordered multilayers, the expected optical properties were calculated using a computer code based on an earlier theoretical paper [18] to account for the multilayer structure and the Maxwell–Garnett theory for the behavior of In particles smaller than the wavelength of the visible light. As seen in Fig. 9 the simulations for the as grown multilayer (In

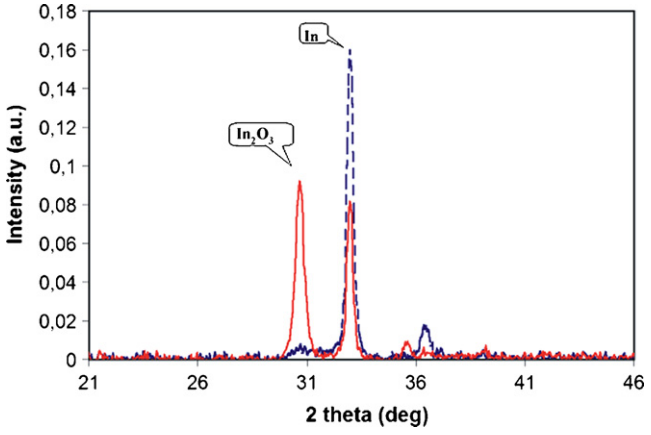

Fig. 6. XRD spectra of the as grown multilayer (blue, thick, broken line) and of the same sample after 30 min annealing in air at 318 °C (red, thin, continuous line). (For interpretation of the references to color in this figure legend, the reader is referred to the web version of the article.)

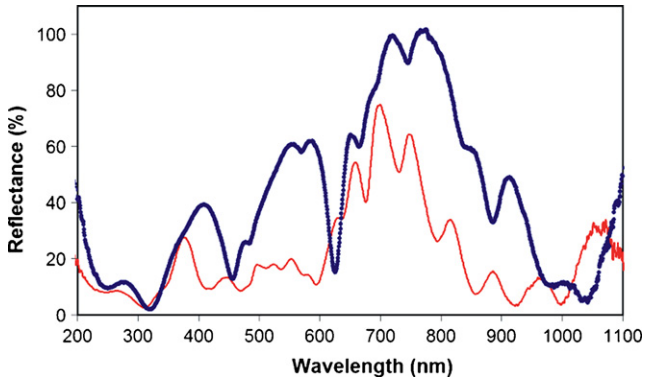

Fig. 7. Normal incidence reflectance spectra measured with respect to an Ocean Optics high-reflectivity specular reflectance standard of as-grown (thick, blue, dotted line) and of the oxidized sample (thin, red, continuous line). One may note the complete disappearance on the annealed sample of the reflectance peak in the range of 500–600 nm. (For interpretation of the references to color in this figure legend, the reader is referred to the web version of the article.)

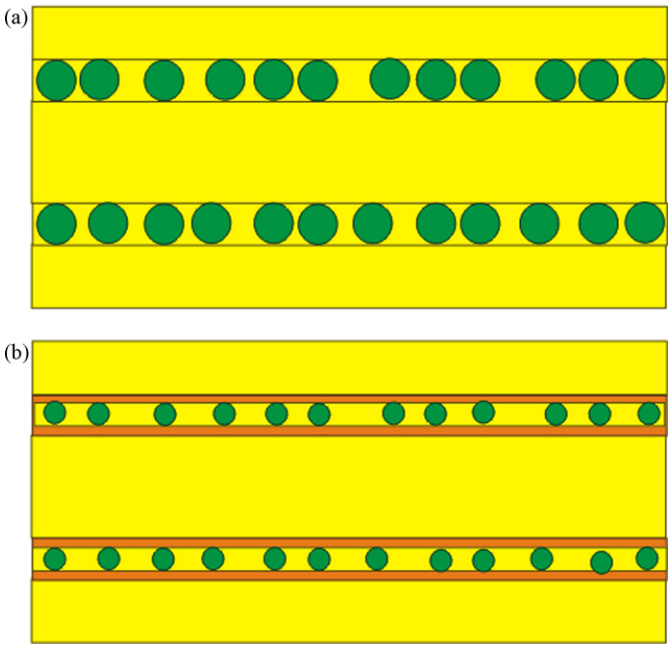

Fig. 8. Schematic drawing showing the oxidation induced modification in the multilayer structure. Light grey (yellow) stands for oxide, dark grey (green) stands for In particles. (a) Before oxidation; (b) after oxidation, the darker bands on the upper and lower side of the In particles denote the widening of the region which contains only oxides. Drawing not to scale. (For interpretation of the references to color in this figure legend, the reader is referred to the web version of the article.)

volume filling fraction equal to 0.2) and for the oxidized case (In volume filling fraction equal to 0.1), respectively, show similar behavior with the experimental curves. The experimental peak for the as grown multilayer is somewhat broader than the simulated one due to the fact that the In nanoparticles are not monodisperse.

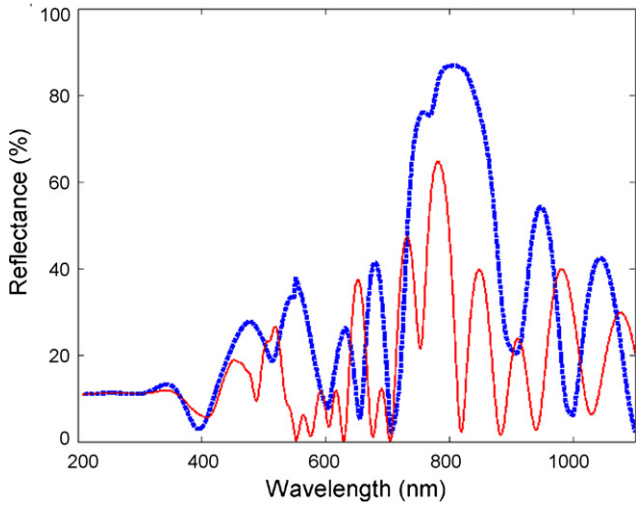

Fig. 9. Simulated reflectance spectra for the as-grown (thick, blue, broken line) and the oxidized (thin, red, continuous) line quasiordered, multilayer nanoarchitecture of In & SiO and SiO. The volume filling fraction values for In are 0.2 for the as grown and 0.1 for the oxidized nanoarchitecture, respectively. (For interpretation of the references to color in this figure legend, the reader is referred to the web version of the article.)

3. Conclusions

The structure of the scales responsible for the coloration of the dorsal (blue) and ventral (green) wing surfaces of the butterfly *A. metallica* were investigated by electron microscopy, optical characterization and image processing. The careful analysis of the nanoarchitectures revealed that quasiordered multilayer structures may behave as photonic band gap materials and produce different colors if the parameters of the local order are different. A successful attempt was made to reproduce the biological template using thin film deposition techniques. It was found that the artificial quasiordered nanoarchitecture, although it has a very different structure from a 1D photonic crystal (Bragg reflector) exhibited clear reflectance maxima, and it was possible to tailor the position of these maxima reducing by oxidation the particle size of the random In inclusions in SiO separating homogeneous layers of SiO.

Our successful attempt to reproduce the color generating, bioinspired nanoarchitectures, by simple and well established, cheap techniques, like thin film deposition, clearly demonstrated the potential of bioinspired designs in various coatings and possibly in other fields like colorants, paper and textile industry.

Acknowledgements

The butterfly specimens used in the present study were donated by the Hungarian Natural History Museum. The work was supported by EU6 NEST/PATHFINDER/BioPhot-012915. The work in Hungary was partly supported by OTKA-NKTH-K67793. The work in Belgium was partly carried out with support from EU5 Centre of Excellence ICAI-CT-2000–70029.

References

[1] E. Yablonovitch, Phys. Rev. Lett. 58 (1987) 2059–2062.
[2] S. John, Phys. Rev. Lett. 58 (1987) 2486–2489.
[3] J.D. Joannopoulos, R.D. Meade, J.N. Winn, Photonic Crystals: Molding the Flow of Light, Princeton University Press, 1995.
[4] A. Arsenault, S. Fournier-Bidoz, B. Hatton, H. Míguez, N. Tétreault, E. Vekris, S. Wong, S.M. Yang, V. Kitaev, G.A. Ozin, J. Mater. Chem. 14 (2004) 781–794.
[5] R.C. Schroden, M. Al-Daous, Ch.F. Blanford, A. Stein, Chem. Mater. 14 (2002) 3305–3315.
[6] A.F. Koenderink, A. Lagendijk, W.L. Vos, Phys. Rev. B 72 (2005), 153102-1–153102-4.
[7] K. Busch, S. John, Phys. Rev. E 58 (1998) 3896–3908.
[8] P. Vukusic, J.R. Sambles, C.R. Lawrence, R.J. Wootton, Proc. R. Soc. Lond. B 266 (1999) 1403–1411.
[9] S. Kinoshita, S. Yoshioka, Y. Fujii, N. Okamoto, Forma 17 (2002) 103–121.
[10] K. Kertész, Zs. Bálint, Z. Vértesy, G.I. Márk, V. Lousse, J.P. Vigneron, M. Rassart, L.P. Biró, Phys. Rev. E 74 (2006), 021922-1–021922-15.
[11] L.P. Biró, Zs. Bálint, K. Kertész, Z. Vértesy, G.I. Márk, Z.E. Horváth, J. Balázs, D. Méhn, I. Kiricsi, V. Lousse, J.-P. Vigneron, Phys. Rev. E 67 (2003), 021907-1–021907-7.
[12] H. Ghiradella, in: M. Insecta, Locke (Eds.), Microscopic Anatomy of Invertebrates, 11A, Wiley–Liss, 1998, pp. 257–287.
[13] D.G. Stavenga, M.A. Giraldo, B.J. Hoenders, Opt. Express 14 (2006) 4880–4890.
[14] L.P. Biró, Zs. Bálint, K. Kertész, Z. Vértesy, G.I. Márk, L. Tapasztó, V. Lousse, J.P. Vigneron, in: P.V. Braun, S. Fan, A.J. Turberfield, S.-Y. Lin

(Eds.), Three-Dimensional Nano- and Microphotonics in Mater. Res. Soc. Symp. Proc., vol. 1014E, Warrendale, PA, 2007, paper: 1014-AA7.8.
[15] L.P. Biró, K. Kertész, Z. Vértesy, G.I. Márk, Zs. Bálint, V. Lousse, J.-P. Vigneron, Mater. Sci. Eng. C 27 (2007) 941–946.
[16] L.P. Biró, Zs. Bálint, K. Kertész, Z. Vértesy, G.I. Márk, L. Tapasztó, V. Lousse, J.P. Vigneron, in: A. Serpengüzel, G. Badenes, G.C. Righini (Eds.), Photonic Materials, Devices, and Applications II, SPIE Proceedings, vol. 6593, 2007, pp. 659318-1–659318-8.
[17] BioPhot Analyzer Software, http://www.softadmin.ro/biophot.
[18] A. Dereux, J.-P. Vigneron, Ph. Lambin, A.A. Lucas, Phys. Rev. B 38 (1988) 5438–5452.